Computational and Constitutive modeling of Bone's Mechano-sensitivity in:
Virtually Repaired Bone vs. Healthy models.

Author: Salman Saghir.

Fall 2015 MS CS&E 00000117195

Supervisor

Dr. Zartasha Mustansar

A thesis submitted in partial fulfillment of the requirements for
Master of Science
In
Computational Sciences and Engineering (CS & E)

Research Center for Modeling and Simulation

National University of Sciences & Technology

May 2019

Computational and Constitutive modeling of Bone's Mechano-sensitivity in:
Virtually Repaired Bone vs. Healthy models.

By

Salman Saghir.

Fall 2015 MS CS&E 00000117195

Supervisor:

Dr. Zartasha Mustansar.

A thesis submitted in partial fulfillment of the requirements for
Master of Science
In
Computational Sciences and Engineering (CS & E)

Research Center for Modeling and Simulation

National University of Sciences & Technology

May 2019

THESIS ACCEPTANCE CERTIFICATE

Certified that the final copy of MS/MPhil thesis written by Mr. Salman Saghir Registration No. Fall 2015 MS CS&E 00000117195 of **RCMS** has been vetted by the undersigned, found complete in all aspects as per NUST Statues/Regulations, is free of plagiarism, errors and mistakes and is accepted as partial fulfillment for award of MS/MPhil degree. It is further certified that necessary amendments as pointed out by GEC members of the scholar have also been incorporated in the said thesis.

Signature with stamp: ____________________

Name of Supervisor: Dr. Zartasha Mustansar

Date: ____________________

Signature of HoD with stamp: ____________________

Date: ____________________

Countersigned by

Signature (Dean/Principle): ____________________

Date: ____________________

Approval

It is certified that the contents and form of the thesis entitled "Computational and Constitutive modeling of Bone's Mechano-sensitivity in: Virtually Repaired Bone vs. Healthy models.**"** submitted by **Salman Saghir** have been found satisfactory for the requirement of the degree.

Advisor: **Dr. Zartasha Mustansar**

Signature: ____________________

Date: __________________________

Committee Member 1: **Dr. Salma Sherbaz**

Signature: ________________________

Date: ______________________________

Committee Member 2: **Dr. Rehan Zafar Paracha**

Signature: ________________________

Date: ____________________________

Committee Member 3: **Dr. Shahzad Rasool**

Signature: _______________________

Date: ____________________________

DEDICATION

I dedicate my thesis to

My Beloved Parents

Certificate of Originality

I hereby declare that this submission is my own work and to the best of my knowledge it contains no materials previously published or written by another person, nor material which to a substantial extent has been accepted for the award of any degree or diploma at RCMS, NUST or at any other educational institution, except where due acknowledgement has been made in the thesis. Any contribution made to the research by others, with whom I have worked at RCMS, NUST or elsewhere, is explicitly acknowledged in the thesis. I also declare that the intellectual content of this thesis is the product of my own work, except for the assistance from others in the project's design and conception or in style, presentation and linguistics which has been acknowledged.

Author Name: **Salman Saghir**

Signature: ____________________

Acknowledgments

First and Foremost, I am very thankful to the Almighty Allah for his countless blessings and utmost guidance.

Then I would like to thank my Parents for all the support and giving me attention to be able to perform this task, and giving me opportunities which I on my own could never have been able to achieve.

Then I would like to thank my supervisor Dr. Zartasha Mustansar of the Research center for Modeling and Simulations (RCMS) at National University of Sciences and Technology (NUST). The door to Ma'am Mustansar office was always open whenever I ran into a trouble spot or had a question about my research or writing. She consistently allowed this study to be my own work, but steered me in the right the direction whenever she thought I needed it and especially for her confidence in me.

Besides my supervisor, I would like to thank the rest of my GEC committee: Dr. Salma Sherbaz, Dr. Rehan Zafar Paracha and Dr. Shahzad Rasool for their insightful comments and encouragement, but also for the hard question which incited me to widen my research from various perspectives.

I must express my profound gratitude to my beloved parents for providing me with unfailing support, continuous encouragement and their endless love throughout my life and especially years of study. Thank you both for giving me strength to reach for the stars and chase my dreams.

A university teaches us manners and compassion, but an institute might be boring on its own, so we need the company of people those people become our friends or teaches us important life lessons, sometimes both. I passed through quite a lot in these two years of NUST met people, learned lessons, made important & helpful friends. For people who taught me lessons I thank you a lot for teaching me important life rules and regulations.

This accomplishment would not have been possible without them. Thank you all of you once again.

Salman Saghir

Table of contents

Contents

List of Figures:

List of Table:

List of Graphs:

Abstract

Bone’s Mechano-sensitivity is a wide area of research in computational mechanics. ***Bone*** cells are capable of sensing and responding to mechanical forces. However, modeling these forces requires a lot of working and assumptions. There is a strong mechanical connection between mechanical signals and bone behavior. Bone behaves strongest in compression and weakest in shear. The forces that are modeled either by using traditional physical testing methods or by using numerical techniques like Finite Elements vary according to the type of geometry and the loading conditions. Intricate geometries end up having complicated force patterns and poor prediction of actual forces if not assumed properly. Some bones break under lower stresses than others, however the repair after the breakage process is important to understand. The healing processes sometimes bring more strength to the structure than the actual one. This could be due to different mechanical forces which fit well than what bone experienced during breakage. This study, therefore looks into how mechanical strength changes after the healing process.

Studying the mechanics of bone are to improve the understanding of how and why bone fracture. From an engineering viewpoint, fractures represent a structural failure of the bone whereby the forces and moments applied to the bone exceed its load-bearing capacity. In this study a positive correlation is carried out using both physical testing method and finite element modeling to investigate the mechanics of bones in terms of its strength, stiffness, behavior and the amount of damage as a result of external loading and vice versa after healing.

Author utilizes a physical testing method (Uniaxial Compression Loading) and Finite Element Modeling on bird bone (Femur) in both healthy and injured conditions. The bone was virtually repaired using image processing to ally with what is available in the literature on healing. The typical stress fracture occurs during load application, this load may produce a shear tension, resulting in eventual random rupture of bone which is the

case in this study as well. Author found out that these compound stress fractures not only weakens the bone resorption process but also decreases the bone deposit mechanisms to heal the bone quickly. Additionally, author inferred that the repaired bone showed half the amount of stresses to that of the healthy bone hence twice the mechanical strength.

Chapter 1

Introduction

1.1 Overview:

In this chapter, the motivation behind this research, research question and objectives have been discussed.

1.2 Motivation:

Bones are complex, structurally as well as functionally. It is typically thought of having two functions: structural support and storage of minerals such as calcium and phosphorous. Bones also offer protection, such as our skull encasing of brains or ribs protecting our heart and lungs. Bone's work together with muscles, tendons and ligaments to allow work done (Mustansar, 2015).

Bones can be stressed during natural physiological activities that we might not know of. Our skeleton makes use of all the bones in the body to generate work done and daily routine activities. Skeleton plays a critical role in bearing stress. Bones act as a lever to help our musculoskeletal system perform a task. According to, Wolff's law, architecture of bone will change with the stress that has been applied to it.

After studying and researching on prosthetics, bone remolding and its pattern. The mathematical values that would justify the strength of fractured and virtually remodeled model bone were not found in the literature. As with the advancement of research in prosthetics, these prosthetics are being manufactured closer to the real bone so this particular field inspired this research on Fractography of the bone and provide data to the science world. So that the bone-like prosthetics can be created which will help the disabled in getting acquainted with the prosthetic limbs more easily and naturally.

1.3 Research Question:

The bone will fracture under certain stresses and the type of fracture that will be induced on the bone will depend on the type and magnitude of force applied to the bone. And when the bone will reconstruct the bone is supposed to have more strength than the healthy bone.

"*Iinvestigating mechanical strength and damage mechanisms in Virtually Repaired Bone and healthy bone using computational mechanics and geometric modeling.*"

1.4 Objectives:

The ultimate objective of this study is to find the mechanical strength of healthy bone and the remodeled bone. This can be pursued by studying the fractography of the bone and testing the bone under mechanical forces and the reaction of the bone under those forces.

Fracture appears in a bone after the muscles and tendons have been stressed out they become fatigued. Muscles are unable to provide support to the bone, so bone faces all the stress that the force is producing to it so, the bone fatigues and fracture is produced. After being fractured the bone needs to be healed/remodeled in order to work and provide support to the human body. The strength of the bone due to this process increases, so the remodeled bone is stronger than healthy bone (Rubin et al., 2002)

1.5 Layout:

The thesis is documented chapter-wise and each chapter discusses and explains the work that has been put into the research with background gathering of the data for the research. Chapter 1 gives an introduction about the research. Chapter 2 creates the background for the research that has been performed and the methods that has been finalized for the research. Chapter 3 is materials and methods that have been used for the process of fracturing a bone and its virtual repair. Chapter 4 discusses the results from the research and how they are interpreted. Chapter 5 is the conclusion and future work from the research.

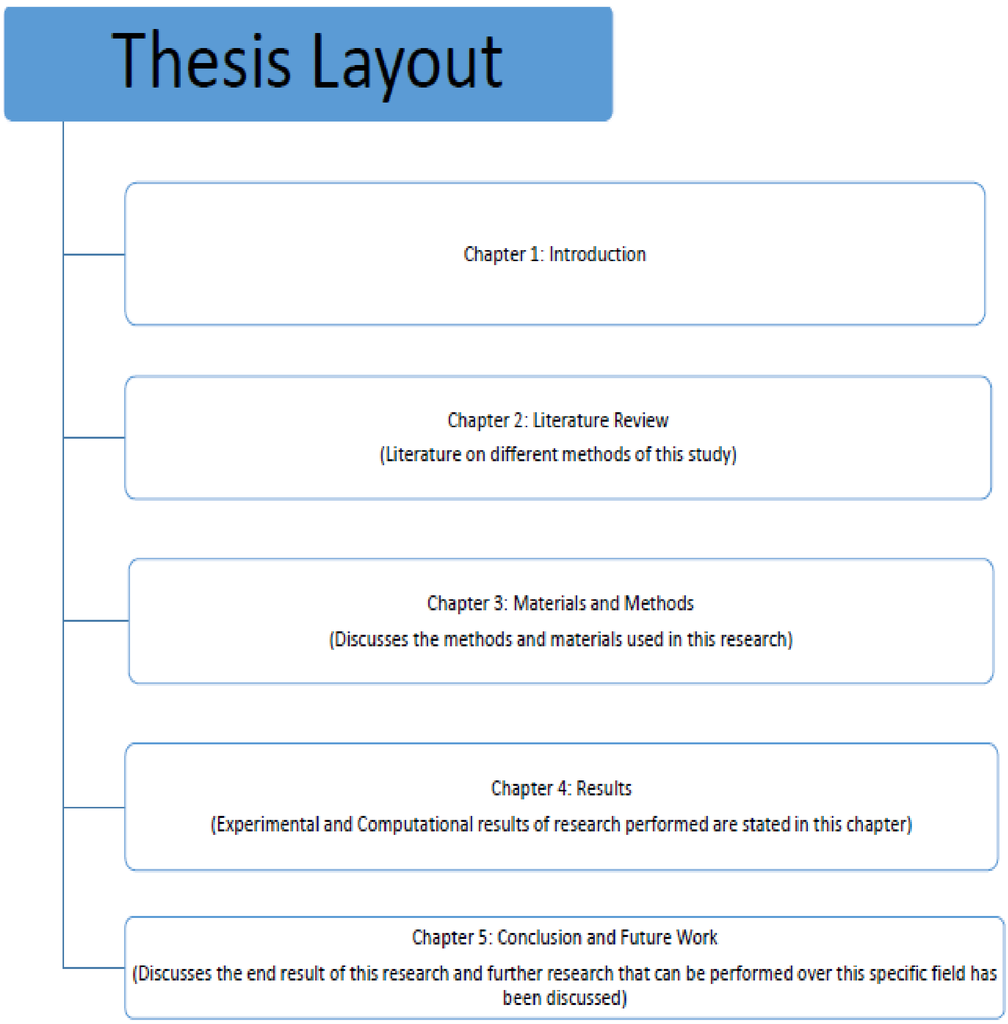

Chapter 2

Literature review

In this chapter the history of Fractography and background that is needed for this research has been developed. Methods that have been previously used on the objects that hold the breaking strength closer to the bone have been reviewed and how those materials reacted under those methods have been discussed.

Fractography is the study of fractures. Fractography helps in understanding the injury mechanism of body, a better performance in terms of strength. Imaging during fractography helps in creating the image based models of bones (digitally). Results from this study helps in the prevention of further fractures and it also helps in the rehabilitation of fractures.

At the near end of 17^{th} century the Guglielmin started the study of cleavage of minerals which is mineral fractography. While at the start of mid of 18^{th} century Haüy noted that cleavage occurred on an airplane. Then this study was taken out for assessment of both quality of metals and effect of alloying metals. Until mid-20^{th} century fractography was used only for alloys, minerals and metals but then this study took a step forward. The scientist started to study the ships and airplanes for fatigue study and how they can prevent the past accidents, also how the vehicle can be robustly manufactured for future. Airplanes such as, SS Schenectady, de Havilland Comet and Boeing-737 played important part in the pioneer study of the fractography in objects other than minerals. Then in the late 20^{th} century the studies were performed on many living things on their movements, their effects on the body.

Following are the fundamental methods that are generally the essence of research on bone's Mechano-sensitivity but their sub-processes are different as it has been shown in the literature survey below:

2.1 Maceration:

Maceration is the process of removing the excess tissue, tendons and muscles from a bone. This process prepares the bone for forensic study and for research purposes. This process is to see how much force a bone can face without its supportive parts.

Although there are many different techniques for maceration, detergent maceration has the lowest health risk to the bone. The acceptable results for forensic purposes were produced by the enzymatic action of detergent maceration (Mairs et al., 2004)

Many different maceration techniques have been performed and compared and the conclusion that bleach maceration is the worst technique for the bone quality and subsequent DNA purity while water maceration is rather cleaner and very small loss of material has been reported (Steadman et al., 2006).

The nuclear aspect amplification of the bone has been suggested to be boosted with microwave maceration or Biz/Na2CO3 in sub-boiling water (Lee et al., 2010). Enzymatic maceration is rather useful maceration in terms of odor and time (Simonsen et al., 2011)

Water maceration causes the bone to either over-cook or soak the water altering the properties of bone unless dried properly. Beetles for beetle maceration are not available everywhere and also there is a need of special environment for them to be kept alive so beetle maceration is inconvenient. During bleach maceration the bones may develop whitening of calcification, which will ruin the sample (Offele et al., 2007, Mann and Berryman, 2012). The microwave oven maceration produced better results in terms of odor, harmfulness and ease of access than other methods (King and Birch, 2015)

In this research, hot water maceration has been used, as this maceration technique includes simple materials as household detergent, water, salt and high temperature for water boiling.

2.2 Physical Testing:

Physical testing of an object will show the strength of the material and will be quite helpful for the research and manufacturing purposes. Following literature review has been collected for choosing the technique for this research.

There is a great influence on the fracture pattern due to grain size, also as the indentation load increases the damage area, indentation area and total damage area increases. As the load increases and the number of cycles produced the highest amount of the accumulated residual strain (Mukhopadhyay, 2001). As the grain size is increased so does the fracture toughness of a material up to 5wt%, then it suddenly drops after 5wt% (Bucevac et al., 2007)

The (initial fracture strength) K_{IC} parameters which are influenced by this process are indentation load, hardness and resulting crack lengths (Shukla and Lawrence, 2010). The grain size of the material does matter to its toughness, reduction in the crack tip stress field and increased the applied stress required for the crack extension is due to wrapping of a material with similar material (Krstic and Krstic, 2012)

Higher the strain rate the smaller the young modulus and yield stress is same for all the temperatures (Liao et al., 2011). The difference in the fracture cross-section between the heated silicon piece and non-heated piece was none and they hold same physical and fractural properties (Kim et al., 2011).

There is no significant difference at 21^0C and 37^0C on the mechanical strength of a bone. Compression tests show a better results than any other mechanical tests as the bone experiences most of the stresses in this test. Although there is a significant strength difference in the time slot of drying of specimens and all show different stress (Sedlin and Hirsch, 1966).

In this research axial compression technique (Ahmad et al., 2007)has been used. As this technique is the ultimate strength test of the bone as in this technique due to the geometrical configuration of bone, it resists against the force that has been applied through both (Upper and lower) condyles of bone.

2.3 Imaging:

To understand and use the fractured bone in a software based environment, there are many methods to capture the image and process it, few of those relevant processes are discussed below.

The probabilistic approach is useful for the modeling of bone's performance (Laz et al., 2007). When the force is being applied to the bone the spatial orientation, loading configuration and specimen shape will define the type of fracture will be produced (Yang et al., 2006). J-integral is a better technique than linear elastic fracture mechanics as it includes both elastic and plastic contribution (Yan et al., 2007).

Intensity Modulated Radiation Therapy (IMRT) is harmful to the sarcoma patients of chemotherapy and periosteal stripping as it increases the fracture risk up to 4% (Song et al., 2006). The effects of registration were measured by the registering a manually validated clinically approved 3-D surface model created through semi-automatic method (Greenspan et al., 2006)

The most reliable method to assess the bone fracture risk due to osteoporosis is X-ray imaging. These images have been studied in the connection with the box, mineral density estimation (Lee et al., 2006). Normal and diseased class of bone minderal density, which are extended by extracting energy, correlating the properties. (Juliastuti et al., 2013).

The ultrasound leads to an earlier onset of angiogenesis and causes an up regulation in VEGF expression and it leads to increases the amount of new blood vessel formation and accelerated bone healing (Vavva et al., 2015). The cortical bone thickness does disperse the guided waves and the frequency velocity spectrum analysis is quite better for analyzing the sensitivity of bones (Tran et al., 2015).

CT scanned images has been used in my research as this the modern composition of X-ray imaging and Ultrasound imaging. Also, it produces 3D images of the bone in better contrast than other techniques and the images generated by CT are easily accessible in software for research purpose.

2.4 Finite Element Method (FEM):

For the division of very complicated problems into the small elements, FEM is used that can be solved in relation to each other. Due to FEM the Partial Differential equations are reduced to a system of algebraic equations which can be solved rather easily. FEM includes the following steps:

- Creating finite elements by discretizing the model.
- Identifying nodes and elements of the model.
- Define material properties
- Apply boundary conditions
- Solve for displacements
- Solving for stresses and element forces.

However, in this research the computational FEM is used and all of these stated steps have been performed computationally. And these steps include:

- Selection of models.
- Assigning of material properties to the model.
- Creation of meshes of the model.
- Assigning boundary conditions to the model.
- Testing that model against the real life forces.
- Analyzing the results stress and strain of that model.

Compression load was the mechanical test and the total reaction force of each loading step was calculated to generate a force-displacement curve. The stiffness, yield load and work to yield were determined for each vertebral body (Matsuda, 2016). Branching behavior and crack propagation depends upon the type of test that has been applied to the object and it has been validated by performing Finite Element Modeling (Werner et al., 2017).

Tetrahedral mesh using high mesh resolution is better choice in FEM yet one of the limitations was that the use of rigid elements creates easiness for load defining process but ends up creating unrealistically high stress for the connecting loads (Campbell et al., 2017).

The Finite Element Modeling is the crucial part of any software based modeling and software based testing as the bone will be tested as original bone by using the same values of young's modulus and Poisson ratio. Tetrahedral meshing with encastre boundary conditions has been used in this research, since tetrahedral meshes are better suited for irregular geometries (Zhang and Fan, 2014) and encastre boundary conditions for the bone will not be moving or rotating in any of the axes namely X-axis, Y-axis and Z-axis.

2.5 Summary of the Chapter:

In this chapter the background for the chosen research question has been discussed and in the further chapters it has been shown that how this literature has helped us in selecting the materials and methods for the research.

Chapter 3

Methodology

The study is in six fold stages. In the first stage maceration has been performed and samples were created for the further testing using tibia from *Gallus Gallus Domesticus*. On the second stage the mechanical testing was performed to produce fractures and in the third stage, those samples were CT-scanned. Then at fourth stage the scanned images were imported into Mimics innovation suite for image processing and at fifth stage Finite Element Modeling was performed in the same software. Finally, on sixth stage the models were imported into the ABAQUS CAE software and then the mechanical testing was performed on the FE models. The software MIMICS 20.0 and Abaqus 16.0 were running on HP notebook with core i5 (6^{th} generation), AMD Radeon Graphics Card 2 GB and RAM 8 GB.

For research purposes, various options were visited for such purpose and as human cadaver bones are quite difficult to acquire and the machine that was available for physical testing did not have such equipment or the capacity to handle such long bone. So it was finalized that the tibia from *Gallus Gallus Domesticus* (Chicken) was selected. The tibia in this specific bird as this is a flightless bird which uses very little amount of its wings. Once the bone was extracted from *Gallus Gallus Domesticus,* it was macerated and then physically broken by compressing the bone in a Universal Testing Machine (UTM) and then it was CT scanned for the analysis. Workflow for this research is shown as Figure 3.1.

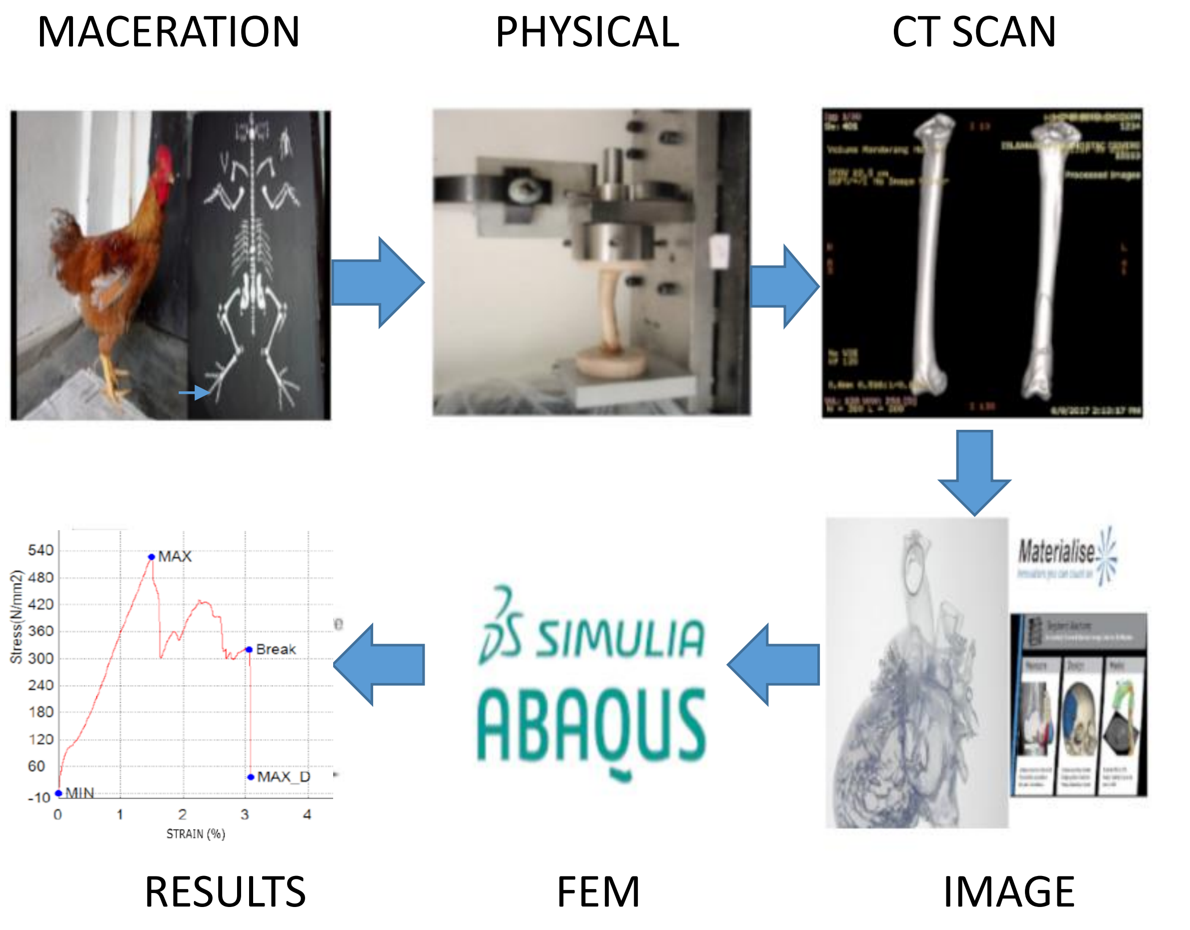

Figure 3.1: WORK FLOW for the Research

Following materials/methods are used in the research.

1. Maceration
2. Mechanical Testing
3. Image acquisition
4. Image Processing
5. FE Modeling

3.1 Maceration:

Removing the flesh, the tissues of a bone is quite a difficult task and there are many methods from which the flesh can be removed as:

1. Hot water maceration
2. Cold water maceration
3. Beetle maceration
4. Bleach maceration

As from section 2.1, each of the process has its own perks. In hot water maceration, bone is kept in containers or hot plate with a solution of water, some chemical salt is added, then it is heated and tissues start to fall off. Then the bone is cleaned using some instrument like scalpel/scissors or brush. In cold water maceration bone is placed in a container with a solution of water, some chemical salt is added and it takes about weeks for the tissues to falloff and then an instrument is used to remove the remaining tissue to clean off the bone. The difference between the two is the time in which the tissues are removed from the bone, hot water maceration takes 4-5 hours while the cold water maceration takes a week or more.

With beetle maceration the bone is placed in a pit of beetles and they eat off the excessive tissues and the bone is acquired clean and no instrument is needed to clean the bone. In bleach maceration household bleach (3-6% sodium hypochlorite) is used and bone steamed for specific time and then the excessive tissues are removed by hands after that the bone is immersed in the bleach for 15-20 minutes and kept on close watch for any formation calcification or whitening of the bones after that the bones are washed with tap water.

3.1.1 Maceration used in this research:

In this process, the sample is taken out of the target and then flesh, tissues and tendons are removed from that extracted sample and thus the sample is prepared for the research. Tibia of healthy chicken *(Gallus Gallus Domesticus)* of 1.8 Kg was obtained and the tissues were removed using Hot Water Maceration. This process took about 4 Hrs. With constant temperature of 125 ^{o}C with addition of simple home used salt (NaCl) and household detergent in the water to remove any left out fat on the bone. After removal of bone from water a simple brush and knife were used to remove any left out tissues and fat from the bone. Then for the next 48 Hrs the bone was placed in open air at room temperature and was thoroughly dried up. Bone before and after maceration is shown in figure 3.2.

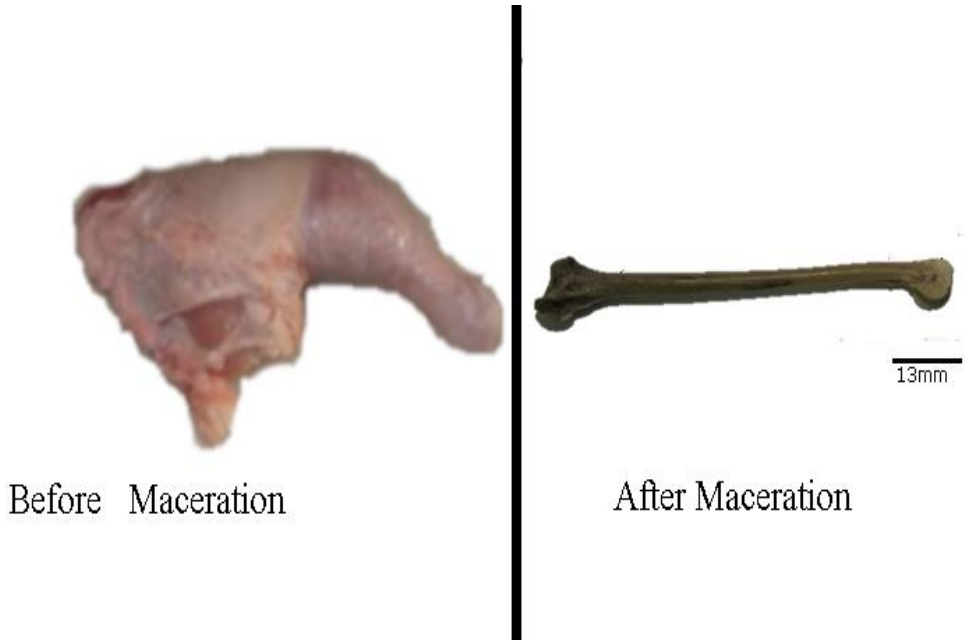

Figure 3.2: Bone before and after Maceration (Muscles, tendons and tissues have been removed through maceration on the right bone)

3.2 Mechanical Testing

Mechanical testing of an object for its durability is quite important. For this purpose many mechanical testing machines and devices are present. Universal Testing Machine (UTM) Shimadzu 20kN (Autograph (AG+) plus) has been used in this research as it can perform mechanical test on small objects like small bones from a small animal. The graphs produced from this machine are very well represented and very interactive. Which helps a lot in understanding the process, mechanical testing on objects. The machine is shown in figure 3.3. This machine has following parts and software for the research purpose.

Figure 3.3: Universal Testing Machine (UTM) Shimadzu 20kN (Autograph (AG+) plus

1. TRAPEZIUM X Software
2. Plastic Bending Test System for JIS/ASTM Standard Compliant
3. Manual, Non-Shift Wedge Grips

Figure 3.4: 3-Point bending apparatus

Figure 3.5: Compression testing apparatus

Manual, Non-Shift Wedge Grips has been used in this research for compression testing. The sample was placed in the upper wedge and was tightened till it wasn't showing any kind of motion in X-axis and Y-axis and similarly it was mounted on the lower wedge. Then incremental load with 0.05mm/sec step was applied on the upper condyle of the bone. After which the bone started to produce the crackling sound as the load increased but nothing was visible, though after reading the graph (refer Graph 4.1) it was understood that the trabecular bone started to produce fracture at 120 N which was the maximum strength of this bone.

The experiment was continued unless a fracture was visible to the naked eye, so after that the bone was still being fractured but only on the trabecular bone, but as the force reached 527 N the creep started to appear on the cortical bone. Then this creep started to grow under fluctuating load and finally at 320 N the bone was fractured and comminuted fracture was induced on the bone due to this experimentation. This whole experiment lasted for 61.73 seconds, then the bone broke off into pieces. Few parts flew off in X-axis, while the motion of the apparatus was in Z-axis fractured parts remained on the apparatus and then the sample was collected manually from the apparatus and was checked for any missing parts.

Figure 3.6: Sample during mechanical testing (Axial Compression being applied to the bone).

3.3 Computed Tomography (CT-Scan):

CT system utilizes X-beams to create better images for the specialist to analyze the bone's contrast, CT and MRI both provide better contrast for the bones and tissues. 3D images are in high demand as they provide better contrast and more realistic interaction with organs and bones even though 2D imaging is present. MRI and CT are used to reconstruct the images of tissues and bones in 3D mode. The current research aims is to reconstruct 3D model of leg bones from its cross sectional CT images.

To analyze a sample on a computer, images are required, and these images can be acquired through X-Ray, CT-Scan, MRI scan and ultrasound. Since X-ray doesn't provide 3-D images, MRI is only affective in muscle mass and ultrasound also provides 2-D images, CT-Scan was chosen for the image acquisition in this research. As CT-Scan provides the 3-D view of the sample and also it provides high resolution images, which are always good for a research purpose. So, after the mechanical testing the bone was taken from CT-Scan and the healthy bone & fractured bone were scanned side-by-side. The specs of CT-Scan machine are as:

Sr. No	Specifications of CT Machine	Values
1	Acquired Resolution	0.625 mm
2	Planes	AXIAL
3	Source to Sample Distance (mm)	1445 mm
4	Magnification	As Req.
5	Source Volatage (KV)	120
6	Current (mA)	250
7	No. of Projections	One
8	No. of Slices	185
9	Initial Angle (Degree/s)	Zero
10	Beam Time (sec)	5.3
11	Filament / Film to be used	Filaments
12	Can Slides be increased?	Yes
13	Cost Per Slide (pkr)	500
14	Total Cost	2500

Table 3.1: Specifications of CT-Machine used for scanning the bones for research.

Note: These configurations are for dead *Gallus Gallus Domesticus*. A live animal and humans will have a different configuration

Figure 3.7: CT-Scanned Images showing the healthy bone and fractured bone. The image on the top is showing the layer based CT image and the image below is the 3-D model created during this process and showing the amount of current and voltage the bones were exposed to during this process

3.4 Geometric Analysis (Image processing).

This image based modeling can be performed via many software like Simpleware and MIMICS. MIMICS 20.0 have been used for this research as this software is very user friendly and it has high end modeling modules.

MIMICS is an image based modeling tool used to create a model, alter a pre-existing model and create meshes in a model. Many of the researchers have created the models for human healthcare and implemented those using MIMICS through a method of hit and trial. This software is quite helpful and useful for virtual testing of different health care devices that may be used by human. Also devices/models can be virtually drawn on this software and can be prepared for different mechanical software for research purposes.

Then these images were imported in MIMICS Innovation suite and then the mask was placed on the region of interest. Then that region was cropped and that region was put through image processing techniques (discussed below):

1. Creation of Healthy Bone
2. Fractured bone and its virtual repair.

3.4.1 Creation of Healthy Bone:

Healthy bone is created by segmenting one of the bone samples from figure 3.7. The process of segmentation is such that the whole of the image was masked and after that mask from the fractured model was removed. After that excessive mask was removed from the base on which the samples were placed for CT-scanning and healthy model was obtained.

After segmentation the healthy model has been imported in 3-Matic for FEM and five samples varying in volume element of the mesh from coarser to finest were created by alternating the number of triangles present in a mesh. This option is provided in the software and as the number of triangles is increased the mesh size decreases and vice versa. Then these models were imported into MIMICS and then saved with “. inp” format for ABAQUS to read them.

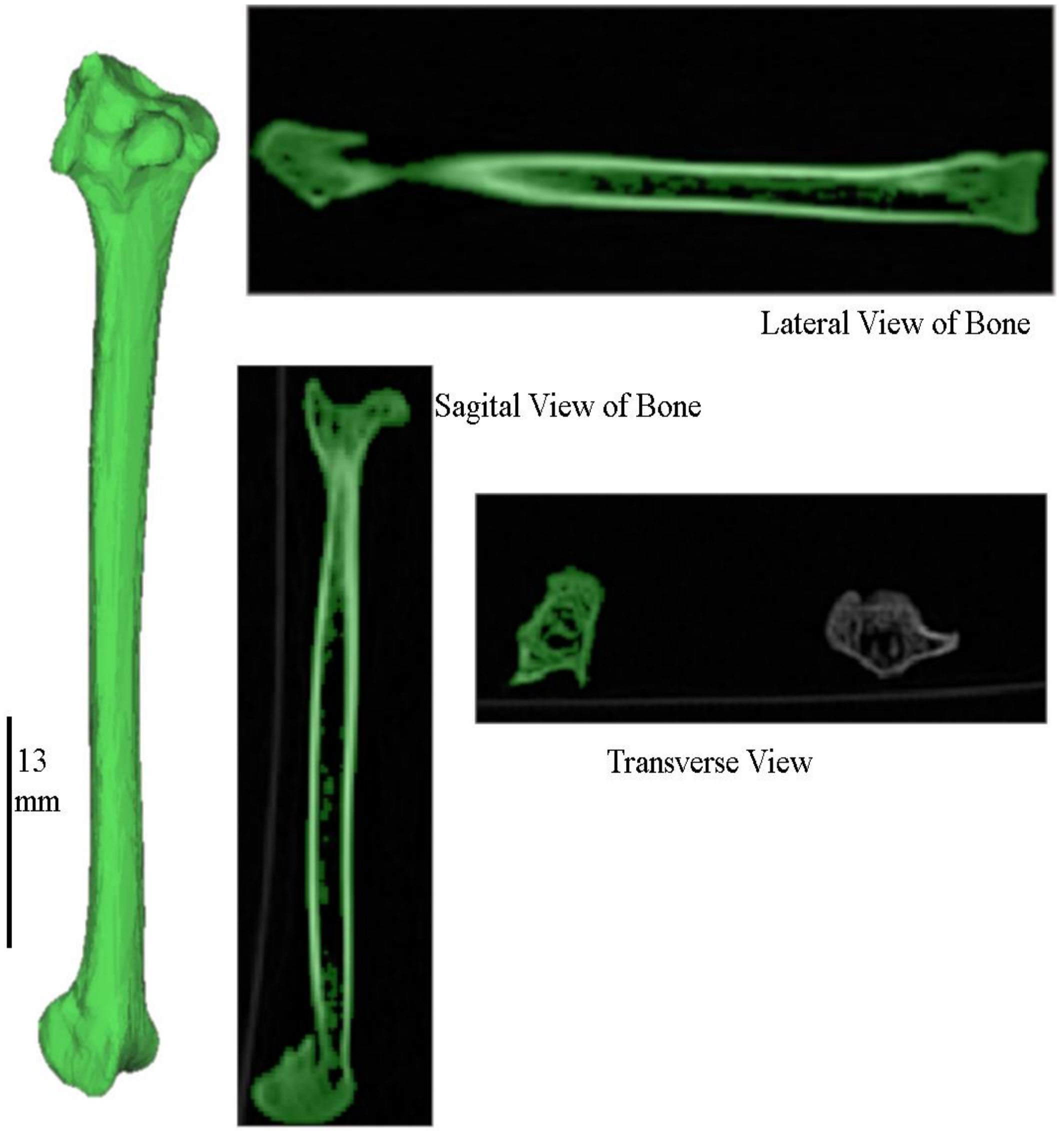

Figure 3.8 (a): Healthy Bone 3-D modeled in MIMICS (Image Segmentation with the Sagittal, Lateral and Transverse views of the bone).

3.4.2 Fractured Bone and its virtual repair:

The fractured bone was repaired using pixel-by-pixel editing of redundant pixels that were not the part of the original bone. The three parts are masked differently because the alignment of the parts of the bone is not possible in MIMICS unless they are masked differently. After being aligned, the parts were merged together and after that, the "wrapping module" in the software has been used to copy remodeling process which increased the thickness of bone.

The sample after that was introduced into the 3-Matic for Finite Element Modeling where five different samples were created with varying in volume element of the mesh from coarser to finer, these were created by alternating the number of triangles present in a mesh. First of all the small number of meshes were generated to create the first model and then further models were created by increasing the number of triangles present in the model by a factor of "2". Then these models were imported back into MIMICS and are saved in ". inp" format for ABAQUS.

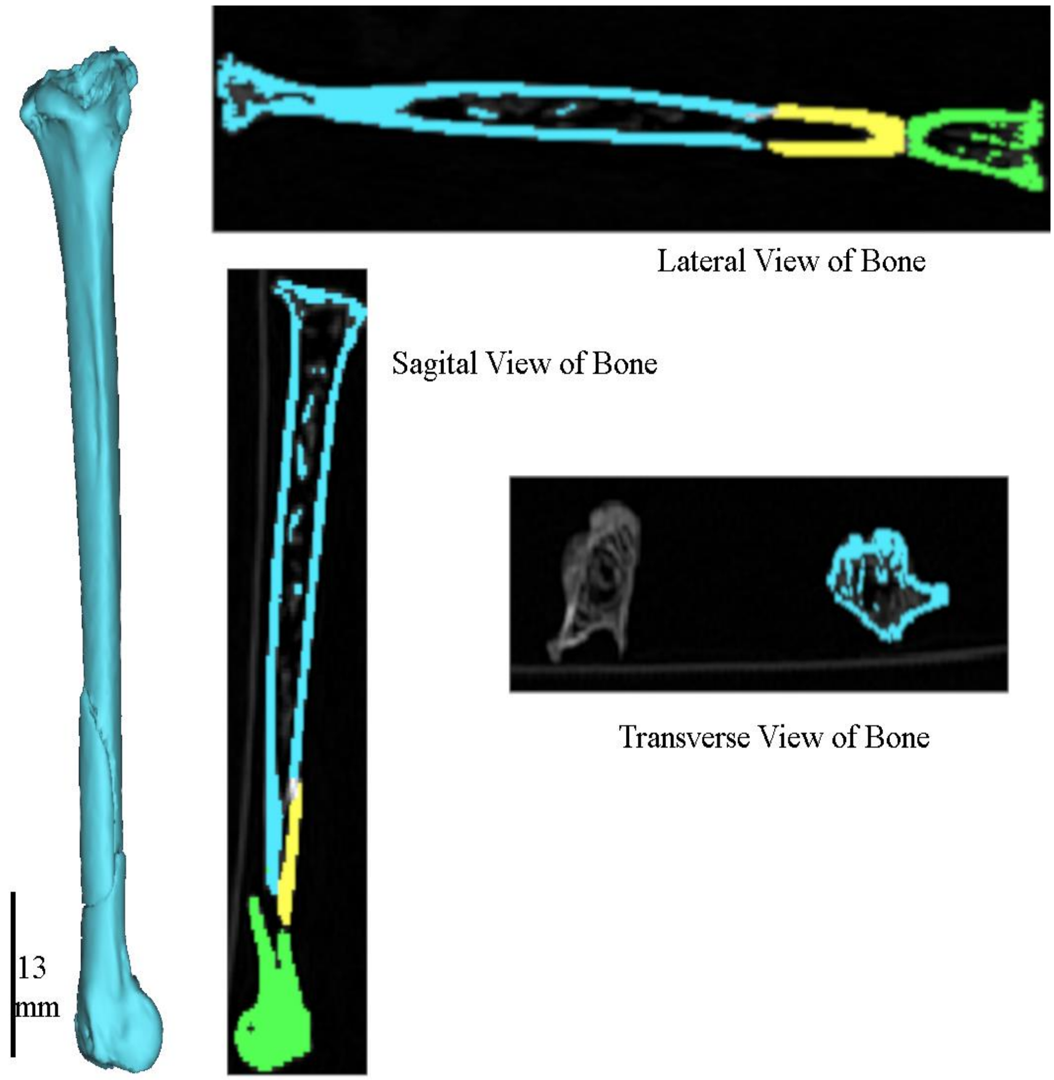

Figure 3.8 (b): Fractured Bone 3-D modeled in MIMICS (Image Segmentation with the Sagittal, Lateral and Transverse views of the bone).

3.5 Finite Element Modeling

FEM has the following steps:

1. Meshing of model.
2. Assigning Material Properties.
3. Applying Boundary Conditions.
4. Load Application.

5. Result analysis.

Mesh was created in 3-Matic of MIMICS Innovation Suite. While the model was assigned material properties, boundary conditions and load in ABAQUS 6.14. Boundary conditions are applied to the lower portion of the bone such that there was no linear or rotational movement in any direction this type of boundary condition is called ENCASTRE, and the load was concentrated force (300 N). The Young's modulus in material properties was taken as "24 GPa" (Reilly and Burstein, 1974, Thurner, 2009).

The tetrahedral meshes were selected for models, they are better suited for irregular geometries(Zhang and Fan, 2014).Tetrahedron have triangular 3-D geometry with base at one end, it has four faces and in meshing it is joined by those faces to other tetrahedrons. So the five models of each bone were generated for the purpose of better analysis and uniformity between the two models. Although the mesh elements in both the models are unlike but the method of mesh generation in both models is identical.

First the normal mesh was auto generated, then the mesh elements were reduced to a point where smaller mesh generation wasn't possible. The first model of each group (healthy bone and virtually repaired bone) had the smallest number of triangles in a mesh. After which the area of each triangle was reduced to get more volume elements in a model and about more than 5-6 models were created to reach the required number of the volume elements in a mesh for each model. After all that the new model for the purpose of better research results was made by going through the same process of reducing the area of triangles in the virtually repaired bone model and from "96k" volume element model "565k" volume elements were generated in the virtually repaired bone model and about 10 models were generated between these two models to get the final mesh. This model with 565k volume elements of virtually repaired bone was finalized for the analysis and comparison of results of healthy and virtually repaired bone models.

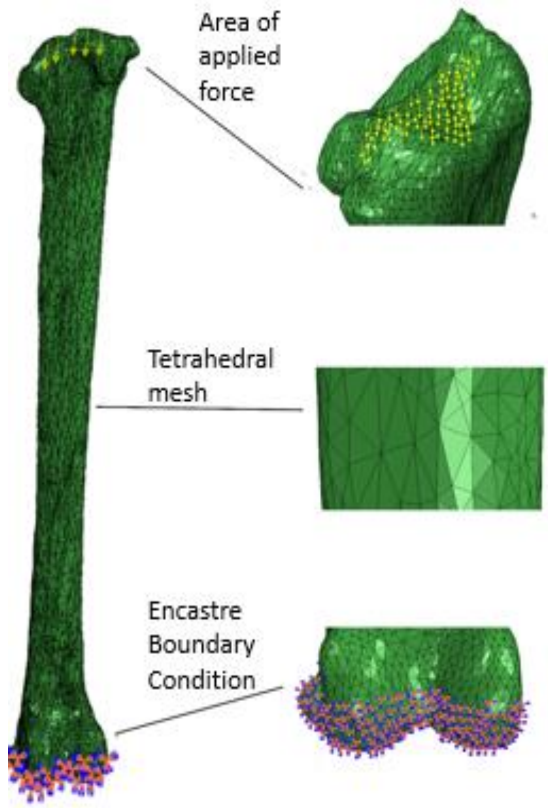

Figure 3.9: Finite Element Modeling and Boundary Conditions (Average Concentrated Forces on two Concave Condyles of the bone with Tetrahedral Mesh& Encastre Boundary condition (Zero movement & Zero Rotation in any direction)).

The average concentrated force was applied on Tibia head at two concave condyles which are articulated with bones of lower leg with incremental pressure '0.50 MPa', '1.0MPa' , '1.5 MPa', '2.0 MPa' , '2.5 MPa' and '3.0 MPa' values. These values were chosen from the experimental data (Graph 4.1). While the model was fixed on 6 Degrees of Freedom (DoF), which means the model is unable to move in X-direction, Y-Direction or in Z-direction and also it cannot be rotated in X-direction, Y-direction or Z-direction, this boundary condition is known as Encastre boundary condition.

The ". inp" files (Refer. In Chapter 3: 3.1.4.2) were imported into the ABAQUS 6.14.2.Then the meshed model has been assigned the material properties. The bone has been assigned young modulus of '24 GPa' (Reilly and Burstein, 1974) which was calculated using:

$$Y = \frac{Stress}{Strain} \qquad \underline{\textit{Equation (3.1)}}$$

Where $Stress = \frac{Force}{Area}, Strain = \frac{Change\ in\ length}{Original\ length}$

And this elastic modulus was confirmed with (Reilly and Burstein, 1974, Thurner, 2009). The Poisson ratio was taken to be "0.3"(Reilly and Burstein, 1975), Poisson ratio is the phenomenon of bone being expanded in the direction perpendicular to the compression.

3.6 Summary of the Chapter:

In this chapter we have discussed the method of maceration used on the bone, physical testing to rupture the bone, Computed Tomography of bone for image processing and using Finite Element Model for virtual mechanical testing.

Chapter 4

Results

The purpose of this research was to study the mechanical properties (Stress vs. Strain) of healthy bone and compare them to virtually repaired bone. This chapter critically discusses the results obtained from this study. Results in detail from maceration, physical testing, image processing and Finite Element Analysis (FEA) have been discussed in this chapter.

The discussions in this chapter are organized as follows:

1. Results from Maceration.
2. Results from Physical Testing.
3. Results from CT-Scan machine.
4. Results from Image processing.
5. Results from Finite Element Modeling.

4.1 Results from Maceration:

The process of removing excessive tissue mass from a bone is quite difficult as the bone must be prepared with complete safety procedure under BioCoshh(Sciences, 2002). Maceration can also alter the bone properties for investigation if not treated using standard safety procedures. Process of maceration is the most efficient for the removal of the tissue from the bone. It helps in forensics and the researchers (Offele et al., 2007, Mann and Berryman, 2012).

Hot water maceration has been selected in this research for feasibility purposes. It took about 4 hours to cook the bone in water, in which household detergent was used about two spoons for removal of any lubrication on the bone and for easy removal of tissues simple home used salt was added in the mix. After that bone has been cleaned and then dried at room temperature for about 48 hours. Figure 4.1 shows the before maceration and after maceration bone.

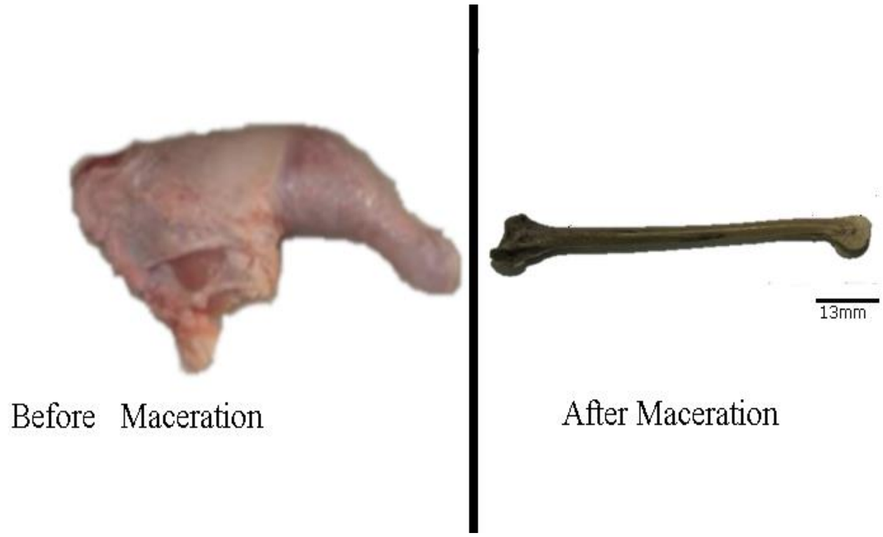

Figure 4.1: Sample after Maceration (Removal of excess tissue from bone).

4.2 Results from Physical Testing:

Universal Testing Machine (UTM) Shimadzu 20kN (Autograph (AG+) plus) installed in the school of chemical and environmental engineering has been used in this research. The specifications of the machine are already mentioned in chapter 3 (section 3.1.2 Page 14). The illustration of stress and strain produced by applying force is shown in the figure 4.2.

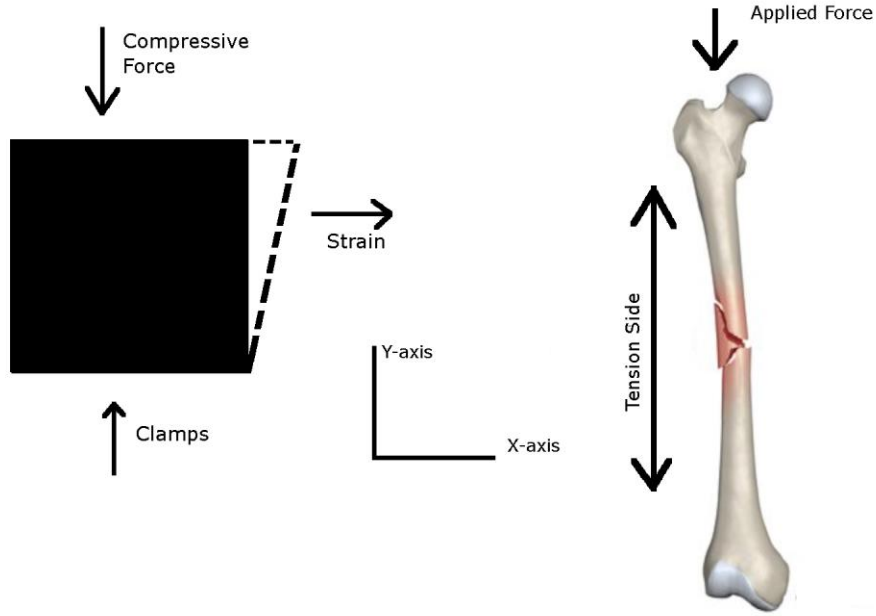

Figure 4.2: Block image is representing the pattern of strain due to the compression being applied to the bone and the bone image is representing how the cracks start to appear on the original bone and the presence of tension due to axial compression –(A) Concept of Force applying on the Bone (B) (loptonline, 2008)

When the force is applied along y-axis, the deformation may occur in x –axis depending upon the boundary condition. In this figure, the object is clamped tightly and there is no space for the object to move along the y-axis. With the continuous application of the force on the bone, the stress on the bone was increased with a coupled tension due to the application of external force. Cracks begin to appear (illustrated in figure 4.2). The bone was fractured in x-axis (as in Cartesian coordinate system) when the bone reached its breaking point during physical testing.

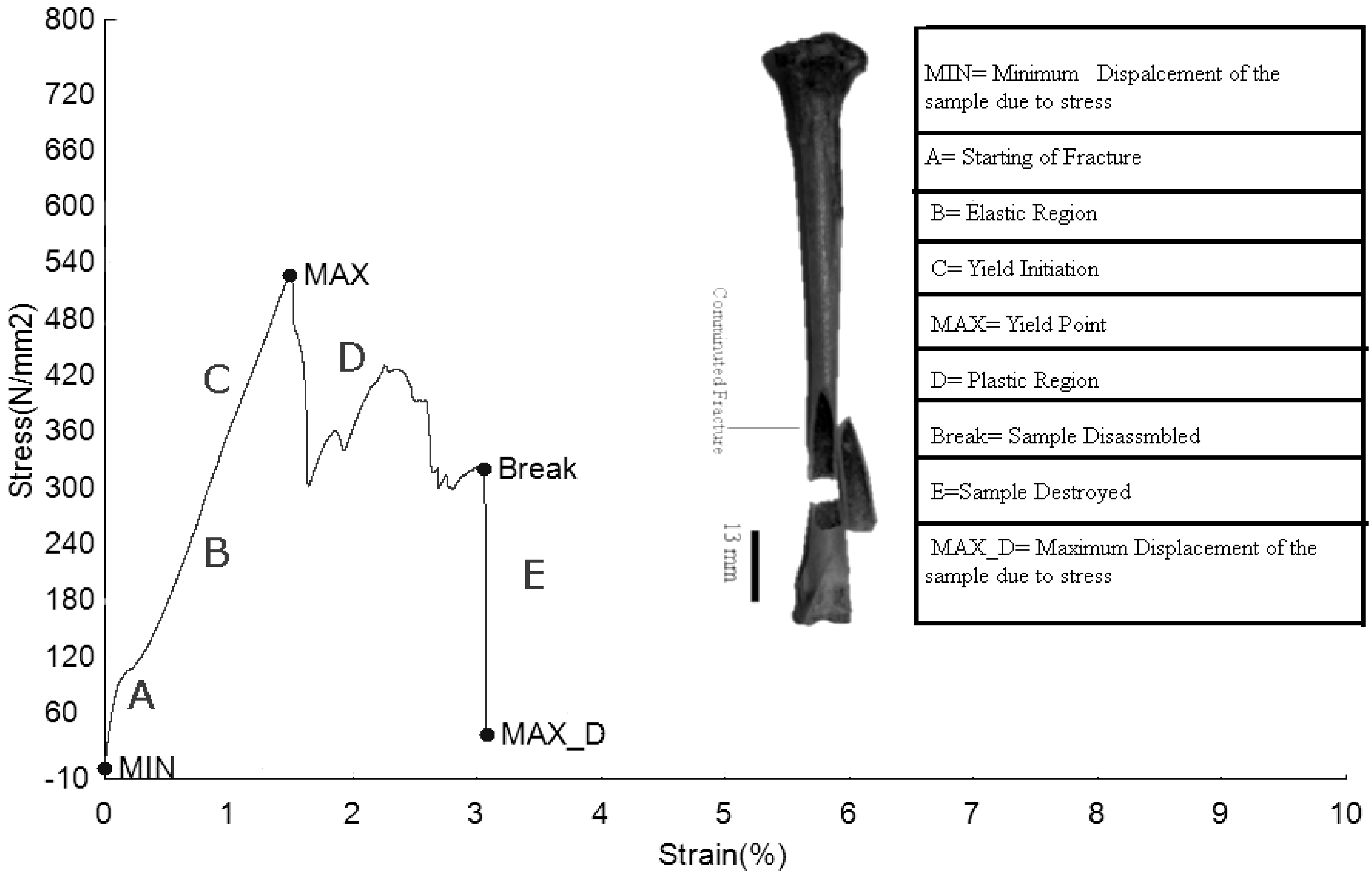

Graph 4.1: Mechanical testing graph (Generated by the mechanical testing machine).

Graph 4.1 is the stress and strain produced in the bone due to the applied force of the universal testing machine. This graph starts at "0 N" force and with incremental force with 0.05 mm/Sec of speed as the force reaches to "115 N" the bone starts to deform as visible from the graph 4.1, the strain on the bone at "115 N" force is 0.2% which is representing the initiation of internal damages in bone. Since bone is still in the elastic region; this means that it has not deformed yet and it can retain its original position if the force is removed. As the force increases the strain increase and the bone proceeds further into the elastic region this graph shows that from "115 N" to "527 N" if the load is removed from the bone before "527 N" force, the bone will be partially functional as the might be a little bent or out of shape but with hairline fractures. At "527 N" the plastic region starts to deform the bone and cracks starts to appear on the cortical layer so the bone will not be able to go back to its original shape even when the load has been removed from the bone.

Yield strain is where the object reaches to the point where the elasticity of the object is finished and plasticity has started while maximum strain is the point where the object totally breaks down. The maximum strain is one-third of the yield strain (Currey, 1988). Plastic region of the graph is showing that as the strain progresses in the bone the force starts to fluctuate and this fluctuation is creating the fractures in the bone a specific manner (observed during experimentation) and as the bone reaches "320 N" the bone breaks forming a comminuted fracture which broke the bone in several pieces "figure 4.2.". Comminuted fracture is mostly splinter/break of the bone into more than two fragments. Since considerable force and energy is required to fracture the bone, fractures of this degree occur after high-impact traumas.

4.3 Results from CT scan and Image processing:

After physical testing the bone was to be regenerated in a software environment and then force was to be applied to it using ABAQUS 6.14. Images from X-ray are in two dimensional while images from CT are three dimensional. Since for computational analysis and image remodeling three dimensional images works perfectly. So CT-Scan was chosen for this research as CT scanned images are far better and easier to model computationally than X-Ray image, also CT-scanned images give a 3D perspective on the sample. For image processing MIMICS software is used and CT images were imported in the software and then the images were manipulated by masking, wrapping and meshing (as explained in section 3.1.4). Following are the images acquired after the whole imaging process:

Figure 4.3: Healthy Model after Image Processing (CT scan of the bone before induction of fracture).

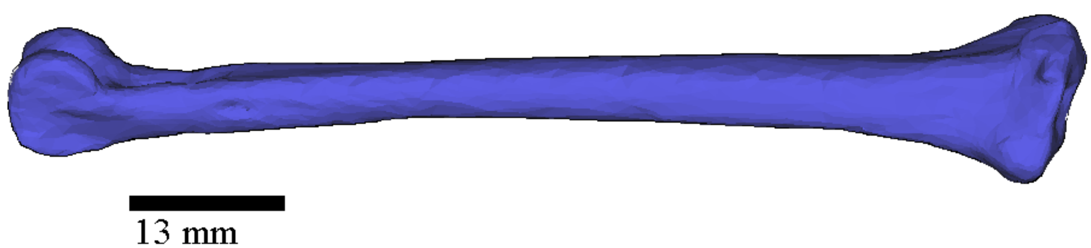

Figure 4.4: Virtually Reconstructed Sample after Fractured (Using Image processing software the sample is reconstructed virtually).

The images of bones are from same, *Gallus Gallus Domesticus* Figure 4.3 is the healthy bone that wasn't fractured and bone in Figure 4.4 is the virtually repaired bone after being fractured.

4.4: Results from FEM (Finite Element Modeling) :

The steps for finite element modeling has been elaborated in chapter 3. The model created/repaired in image processing is meshed, given boundary conditions and load points were also assigned to the upper condyle of bone (See chapter 3 for details). In this chapter the results after compression are being discussed. The following table is for the reference of model volume elements:

Sr. No.	Volume elements of healthy models	The names assigned to healthy models	Volume elements of Virtually Repaired Bones	The names assigned to Virtually Repair Bones
1	36k	MH1	6k	MF1
2	72k	MH2	12k	MF2
3	144k	MH3	24k	MF3
4	288k	MH4	48k	MF4
5	565k	MH5	96k	MF5
6	N/A	MH6	565k	MF6

Table 4 (a): Assigned names of the models.

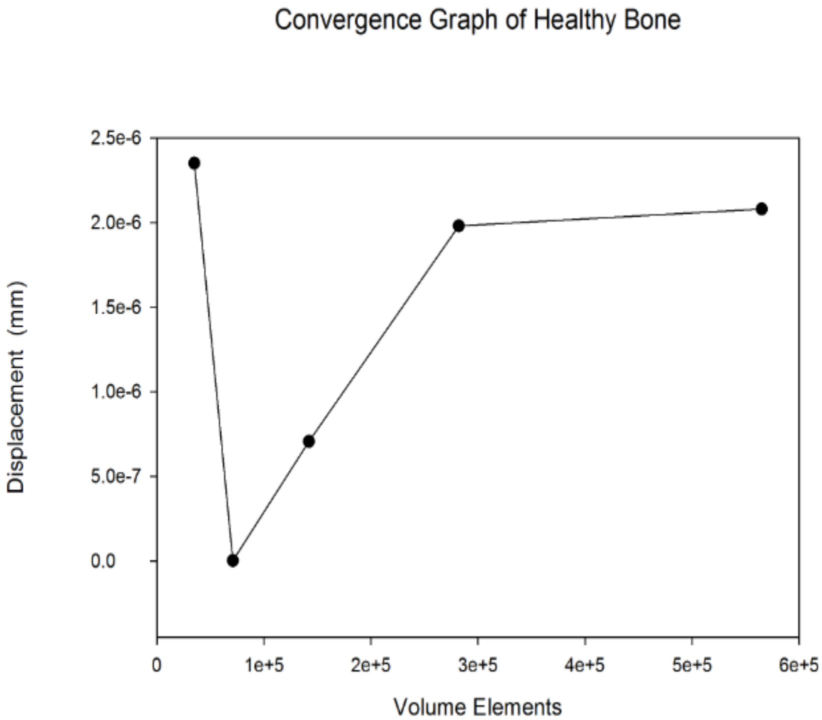

Graph 4.2(a): Convergence Graph of Healthy Bone Model.

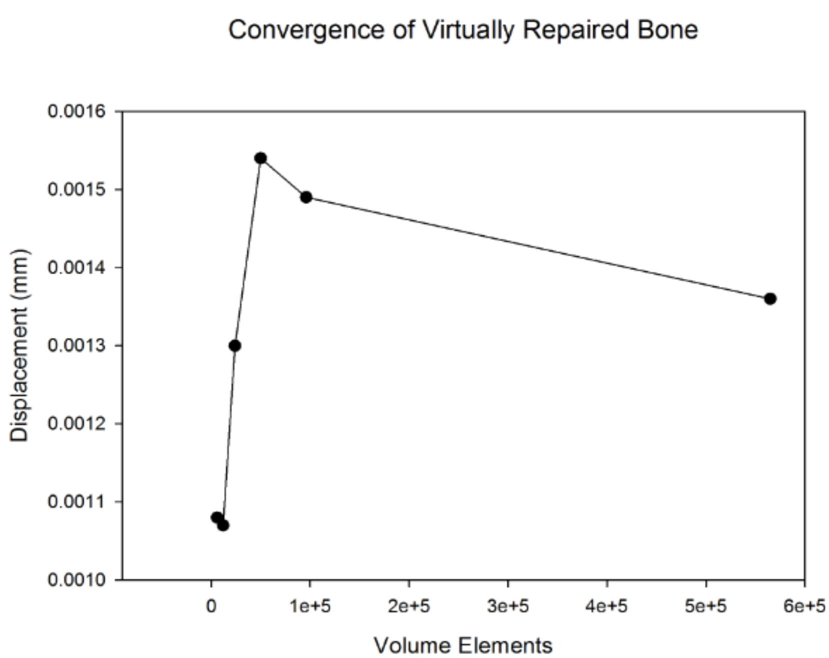

Graph 4.2(b): Convergence Graph of Virtually Repaired Bone Model.

The graph 4.2 shows the relationship of displacement (distance covered by bone due to force applied to it) and the number of mesh elements of healthy bone and virtually repaired boneS. This graph represents the convergence of the displacement with increasing mesh density on healthy model and the virtually repaired bone model. Since MH5 has the maximum amount of mesh elements that can be generated on this specific healthy bone model.

Graph 4.2 shows the convergence pattern of both bone models. So the five models of each bone were generated for the purpose of better analysis and uniformity between the two models. Although the mesh elements in both the models are unlike but the method of mesh generation in both models is identical. First the normal mesh was auto generated, then the mesh elements were reduced to a point where smaller mesh generation wasn't possible. The first model of each group (healthy bone and virtually repaired bone) had the smallest number of triangles in a mesh. After all this process, the similarly mesh of virtually repaired bone model as that of the healthy bone model was created so the results will be comparable and viable for research.

Then the number of triangles was multiplied by a factor of "2" for larger models until five models were created. These five models were created for the convergence, in which the best suitable model for research is carefully chosen by analyzing the pattern of the strain among the different models using same applied force. As a mesh is made finer, the computation time increases, therefore there needs to be a trade-off between the numbers of element mesh has and stress results.

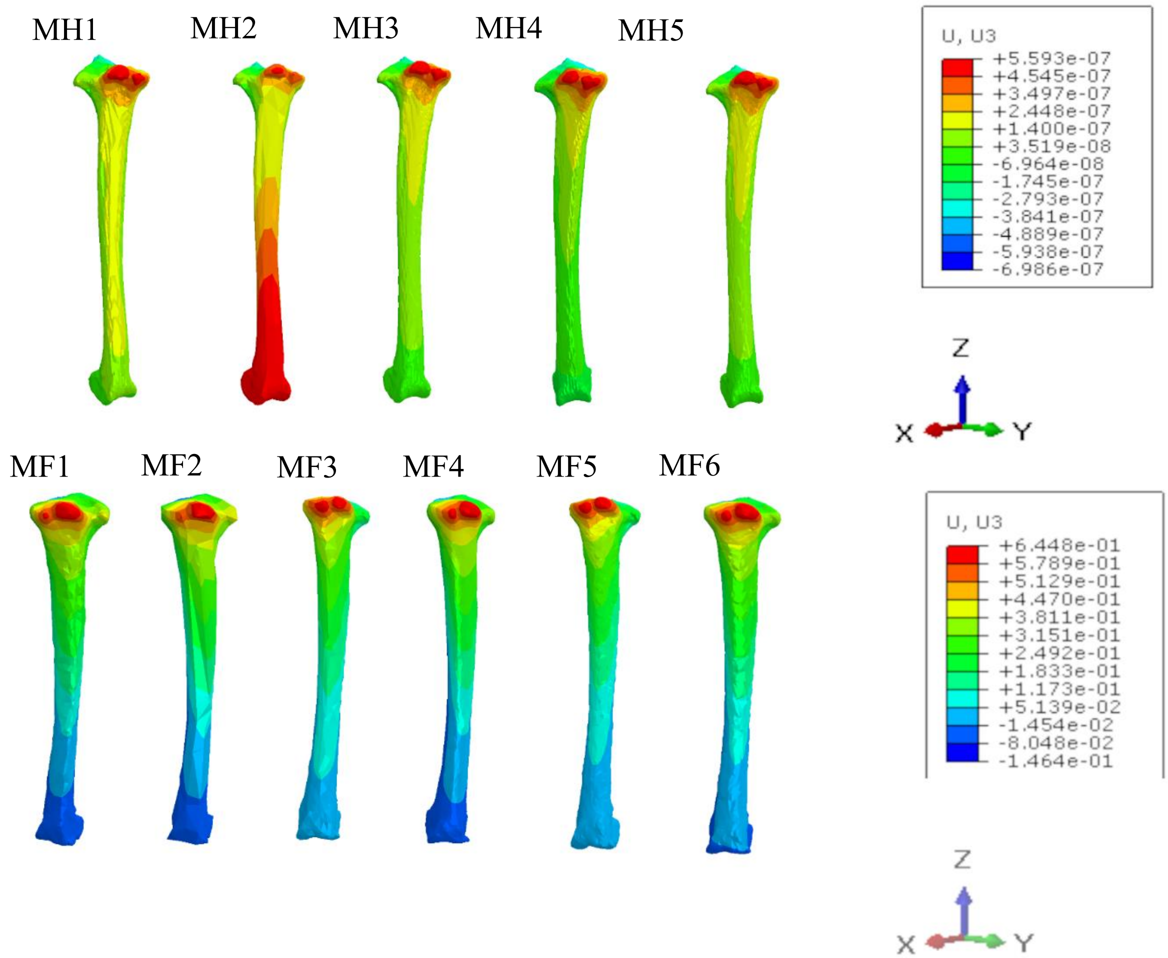

Figure 4.5: Model Convergence (5 models of Healthy and 6 models for virtually repaired fracture bone model are mechanically tested in software and the convergence was observed)

After applying the pressure of '3 MPa' on all the models, the models were compared and analyzed for convergence using the contours of strain on these bone models. The bones from "MH1" to "MH5" are the healthy models on which the pressure of "3 MPa" has been applied (value of force is taken from Graph 4.1). The pattern these bones are showing to the same force is quite peculiar, the strain in higher meshes is small as compared to the strain in lower meshes as shown in Figure 4.6. The bone model "MH1" and "MH2" are showing that the strain due to stress is quite high in these two models, but as we move from "MH3" to "MH5" the pattern of strain starts to lower down and in "MH4" and "MH5" the strain is approximately similar. So the strain has converged on model "MH5" and is chosen for this research.

As in Figure 4.5, the pattern of convergence has been shown with Elastic Modulus of “24 GPa” (Reilly and Burstein, 1974, Thurner, 2009) and Concentrated Force of “300 N” (Graph 4.1). The contours show the convergence pattern of the models, the tables show the range of strains that appeared after force applied to the models. The bones from “MF1” to “MF6” are the Virtually Repaired Bone, bones that have been virtually repaired using MIMICS software and then the force of “300N” has been applied to these bones (value of force is taken from Graph 4.1).

The pattern these bones are showing to the same force is quite peculiar as the mesh elements are increased the strain caused due to stress is decreasing as shown in Figure 4.5. The bone model “MF1” and “MF2” are showing that the strain due to stress is quite high in these two models but as we move from “MF3” to “MF5” the pattern of strain on “MF3” and “MF4” are exactly the same. Which is the strain convergence pattern that was needed to choose the model for the stress test and analyzing for the research. So converged model “MF4” is chosen for this further research. After experimenting with “MF4” the results were not viable as the mesh elements were not as similar to “MH5” so the results from “MF4” were discarded and new mesh were created for virtually repaired bone to be of same volume elements of “565K triangles =MF6” as that of Healthy model so the results will be viable and comparable for further research.

The following graphs show the stress and strain on the selected model. The pressure applied to the models are “0.5 MPa”, “1.0 MPa”, “1.5 MPa”, “2.0 MPa” , “2.5 MPa” and “3.0 MPa”. These forces are selected from the analysis of “Graph 4.1” at 115 N/3.0MPa is the maximum force/pressure that the bone was facing so this is the force to be considered for the research. After that the yield point was taken from the graph as this is the point where the bone started to deform. Then the forces in elastic region were selected and converted into pressure by solving them using following equation:

$$Pressure\ (P(MPa)) = \frac{Force\ (N)}{Area\ of\ Applied\ Force\ (mm^2)} \quad \text{………... Eq (4.1)}$$

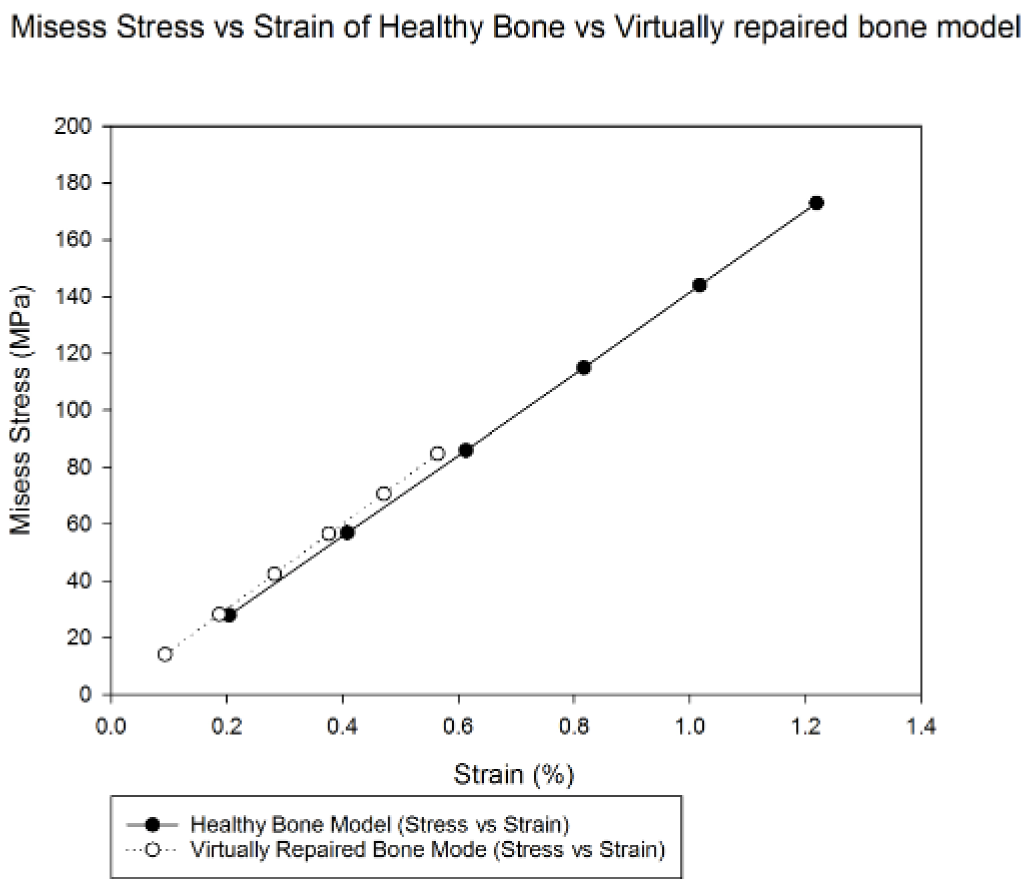

Graph 4.3: Misses Stress vs. Strain pattern: Healthy bone vs. Virtually Repaired Bone

The Graph above is representing the stress patterns of healthy bone in comparison to the Virtually Repaired Bone. The force on the bones is same as it can be seen in the graph, but the pattern and stress on that similar force are different on both of the sample. At 0.5 MPa Pressure the healthy bone is facing 28 MPa von mises stress while the virtually repaired bone is facing 14.14 MPa of von mises stress, this difference in von mises stress of bones is showing that virtually repaired bone is more elastic than healthy bone. The next applied Pressure on the bones is 1.0 MPa and the von mises stress on healthy bone due to this pressure is 57 MPa while Von mises stress on Virtually Repaired Bone is 28.28 MPa.

When 1.5 MPa pressure is applied to the models the Virtually Repaired Bone faces a misses stress of 42.43 MPa while the healthy bone is facing stress of 86 MPa. It can safely be said that in light of these results the Virtually Repaired Bone is more elastic and is less likely to be fractured if compared to the healthy bone on similar forces. These results show that the Virtually Repaired Bone, in this specific scenario, is stronger than healthy bone.

Stress and Strain Values: Healthy Bone and Virtually Repaired Bone				
	Healthy Model		Virtually Repaired Bone	
Pressure (MPa)	Misses Stress (MPa)	Strain (%)	Misses Stress (MPa)	Strain (%)
0.5	28.00	0.204	14.14	0.093
1.0	57.00	0.408	28.28	0.187
1.5	86.36	0.613	42.41	0.282
2.0	115.25	0.817	56.65	0.376
2.5	144.95	1.017	70.69	0.471
3.0	173.71	1.219	84.83	0.564

Table 4.1: Applied Force, Stress and Strain values: Healthy bone and Virtually Repaired Bone.

The Virtually Repaired Bone has been virtually repaired using MIMICS by wrapping layers of material with similar elastic modulus to that of bone as the osteoclasts and osteoblasts envelops the Virtually Repaired Bone to repair it in natural process. Which is the reason why healthy bone is facing more stress and strain than the virtually repaired bone under similar loads.

Applied Pressure (Mpa)	Healthy Model 565K VE	Misses Stress (Mpa)	Strain (%)	Virtually Repaired Bone 565k VE	Misses Stress (Mpa)	Strain (%)
0.5		28	0.204	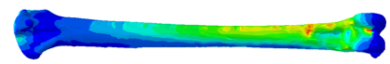	14.14	0.093
1.0		57	0.408	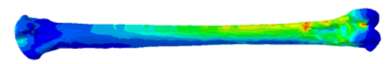	28.28	0.187
1.5		86	0.613	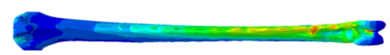	42.41	0.282
2.0		115	0.817	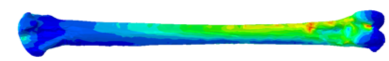	56.695	0.376
2.5		144	1.017	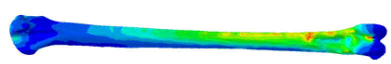	70.69	0.471
3.0		173	1.219	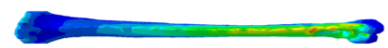	84.83	0.564

Figure 4.6: Stress Plots of the Healthy Vs. Virtually Repaired Model

The "Figure 4.6" shows the stress pattern of the converged models, in which elastic modulus is "24 GPa" (Reilly and Burstein, 1974, Thurner, 2009) and applied forces have been explained in Table 4.1. The stress plots are comparing the stresses of healthy bone model with the virtually repaired bone model. The contours in the figure are representing the areas with higher stress values corresponding to the applied force. The virtually repaired bone model is more elastic than the healthy bone model as it is facing less stress than the healthy bone model at similar applied force.

In latter healthy bone models, the stress is very high on the shaft of bone model near lower condyle. Which means if healthy bone model is going to fracture, it will be around this area of shaft near the lower condyle. While on the similar force in virtually repaired bone model the stress is pretty small and there is no indication as to where the bone may fracture. So the virtually repaired bone is stronger than the healthy bone as shown in figure 4.6 since the virtually repaired bone is more elastic than the healthy bone.

The stress plot comparison of the bones at similar mesh elements will be very useful in study and will provide credible results during comparison of both bone models. As in the figure 4.6. The stresses on the virtually repaired bone is much less than the healthy bone stresses on the similar applied forces. The reason for low stresses on virtually repaired bone is that the bone is wrapped in a material which has similar young's modulus as the bone and it has more of the bone material than the healthy bone to resist the applied forces. So the stresses generated in the virtually repaired bone are very smaller than that of healthy bone. Following is the comparison for the stresses produced on the bone models with similar volume elements.

Pressure (MPa)	Stress on healthy bone model (MPa)	Strain (%)	Stress on Virtually repaired bone (MPa)	Strain (%)
3.0	173	1.219	84.83	0.564

Table 4.2: Comparison between stress and displacement between the healthy bone model and virtually repaired bone model having 565k volume elements

In table 4.2 the comparison between stress and displacement between the healthy bone model and virtually bone model having 565k volume elements of each model. The reason for choosing this specific force is that the stress generated in the healthy bone is still in the elastic region and the bone is going to break after "3.0 MPa" as the stress generated after this force on healthy bone is quite higher than the breaking strength of bone (as from Graph 4.1). The stress generated on virtually repaired bone is about $1/4^{th}$ than the stress generated on the healthy bone model, it is because the virtually repaired bone has sheath of bone due to repairing mechanism around it and the resistance for the applied forces is larger than the healthy bone model. Similar is the case in the displacements the displacement in the virtually repaired bone is quite lower than the healthy bone model for the same reason of virtually repaired bone model has been wrapped in the sheath of bone material for the purpose of repairing the fracture.

The graph 4.4 is representing the age and breaking strength of *Gallus Gallus Domestics* Tibia taken from the literature and also from physical testing. Breaking strength of 320 N at 8 weeks old *Gallus Gallus Domesticus* is observed from physical testing while Breaking strength of 182 N in 4 weeks old *Gallus Gallus Domesticus*, breaking strength of 100.86 N at 3 weeks old *Gallus Gallus Domesticus* and breaking strength of 68.5 N at 2 weeks old *Gallus Gallus Domesticus* are taken from literature (Shastak et al., 2012, Luo et al., 2013).

The pattern in graph is showing the Breaking strength of Tibia in the same species of bird during different ages. Although the breeds are different, but this fact doesn't appear to have any effect on the breaking strength of tibia rather the age and the geometrical details appear to be affecting the strength of bone. The bone in 2 weeks old is 5.21 cm in length, in 3 weeks 6.27 cm in length, in 4 weeks 7.33 cm in length and in 8 weeks old 11.5 cm in length. This increment in the length of bone is also incorporated to the results as the tibia in 2 weeks old *Gallus Gallus Domesticus* is 5.21 cm in length while in 3 weeks old it is 6.27 cm in length and if it keeps on increasing at the rate of 1.06 cm each week the same bird will have 11.5 cm long tibiae by the end of 8^{th} week which is the length of tibiae of the *Gallus Gallus Domesticus* that have been used in this research.

Breaking strength of *Gallus Gallus Domesticus* Tibia			
Breed	Age	Physical testing	Literature
Home-bred	8 weeks	320 N	-
Broiler	4 weeks	-	182 N
Broiler	3 weeks	-	100.86 N
Broiler	2 weeks	-	68.56 N

Table 4.3: Breaking strength of Gallus Gallus Domesticus Tibia from physical testing and literature

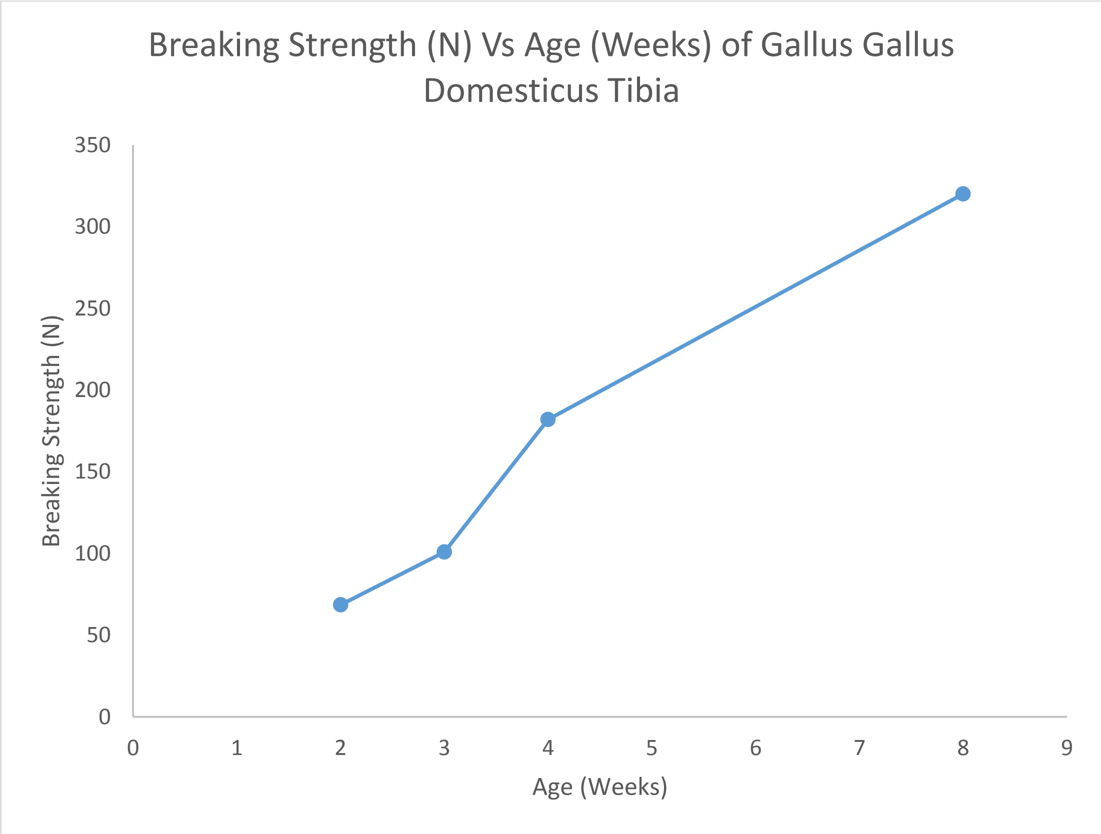

Graph 4.4: Breaking Strength (N) Vs. Age (Weeks) of Gallus Gallus Domesticus Tibia

The *Gallus Gallus Domesticus* with 4 weeks of age has a breaking strength of 182 N and if the value of breaking strength is doubled, it is 364 N which is quite near to breaking strength of the tibia that has been used in this research as the age is almost double the value of breaking strength also seem to have been doubled.

These results from (Luo et al., 2013, Shastak et al., 2012) shows that if the bone keeps on increasing in size then in 8^{th} week the bone would be 11.5 cm long and that was the exact same length of the bone used in this research. So the mechanical properties might also be on the similar pattern as the results from physical testing.

4.5 Result Comparison (Physical test vs Simulated test) :

The results from physical testing were compared to the results from simulations to review the difference between stress and strain (%) of the bone. Following graph will show the difference:

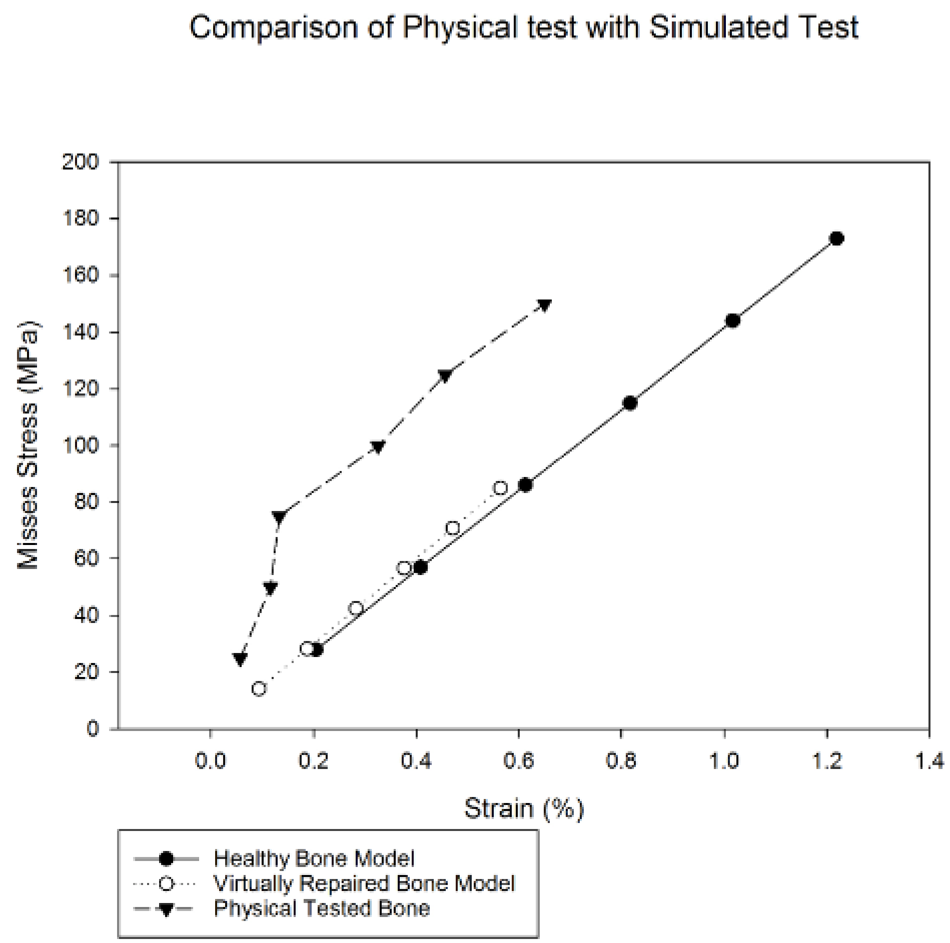

Graph 4.5: Result comparison between physical mechanical testing and simulated mechanical testing (Stress vs Strain of both test are compared in this graph)

As represented in the graph above the dotted line with triangular marks represents the stress vs strain from the physical mechanical tests. The solid line with filled circle is representing the simulated results of healthy bone model. The dotted line with non-filled circular marks is representing the simulated results from virtually repaired bone.

While comparing simulated results by themselves, the stress generated due to applied pressure on the virtually repaired bone is approximately half of the stress generated in the healthy bone model. Similarly, the strain generated in the virtually repaired bone model is approximately half of the strain generated in the healthy bone model.

Although the stress and strain generated in the physical mechanical test are also approximately twice in value to stress vs strain of the virtually repaired bone. Which shows that the simulated results and physical results are nearly comparable during a research. Since the stress generated during physical tests of the healthy bone and simulated results of the healthy bone are approximately similar (some error may be generated during the process due to human/source error).

Although the strain of the healthy bone during the physical test can be compared to the strain generated during simulated results of the virtually repaired bone. This may be the reason that the healthy bone during physical test and virtually repaired bone during simulated results are same bones.

4.6 Summary of the Chapter:

The applied compression concentrated force on the bones is generating stress on healthy and virtually repaired bones. The comparison of applied force and stress between healthy bone and virtually repaired bone is clearly showing that the virtually repaired bone is stronger in the mechanical aspect than the healthy bone. All the graphs and figures are showing the stress generated on the bones due to predefined concentrated forces. From the data it is being concluded that the virtually repaired bone is more elastic as it has less stress generated on it on the same forces as that of healthy bone.

Chapter 5

Conclusion & Future Work

The approach used in this research is quite different from conventional research methods. Physical testing has been performed on bone to create samples and then through the process of image processing and Finite Element Modeling fractured bone has been virtually repaired. The virtually repaired bone has been processed through mechanical testing via computer solver. After which the results have been tabulated and verified by comparing the virtual and physical stress values of the healthy bone.

Computational mechanical test save a lot of time since there is no animal dealing in the lab. Also the wear and tear of bone is a lifelong process and using the virtual data, we ensured that the model will not change in any way unless the changes were performed. Through the virtual repair mechanism it was possible to determine the strength of healed bone and compare it to the physical results of healthy bone for verification.

5.1 Conclusion:

1. Computational Bone Modeling is inferred to be an unprecedented technique to assess the repair and healing strength of fractured bone. This might be later used for clinical prognosis.
2. We conclude that fracture healing is a natural process. Additionally, it restores the mechanical integrity of bone and is greatly influenced by the prevailing mechanical environment.
3. An effort has been made to develop a synergy between mechanics and biology of fractured bone after a computational fracture repair.

4. The strain numbers obtained from this research could be employed clinically. Since the refined models of basic anatomy has been utilized to study the strain fields within a fracture, therefore the approach may be adapted to models for case-specific simulations as well. This may provide a more accurate examination of the relationship between strain and fracture healing in actual patients since the bone basic anatomy is same in all the vertebrates.

5. Our Computer models could also be utilized as teaching models to gain insight into the mechanics of healthy, fractured and fracture-repaired bone.

6. Research finally concludes that stress generation in fracture-repaired bone is halved compared to the applied pressure. The pattern of stress generation under similar load is twice on the healthy bone as compared to virtually repaired bone as much of the applied pressure. So the virtually repaired bone is stronger in terms of mechanical strength to the healthy bone.

5.2 Future Work:

In future

1. Adding muscle mass may make the results more realistic
2. Static analysis is performed in this research. Dynamic analysis can be incorporated as well.
3. The study can also be re-utilized for the study of material properties using L-D curve data.

ANNEX – A

Some experiments are performed to make a pathway for further investigation following experimentations were performed on different bone models. Following models were discarded as the results weren't viable with these volume elements so these results were replaced with the volume elements which were similar in both models.

Stress on 50,000 Volume Element Sample

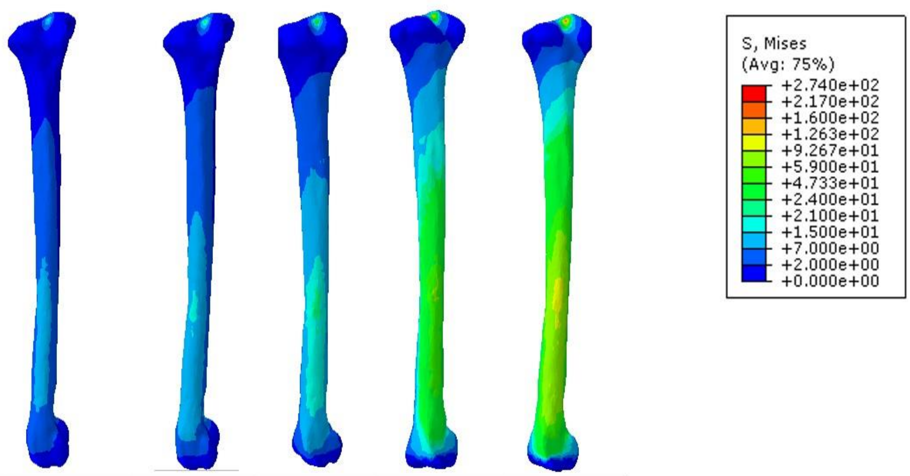

Force (N)	50	82.5	115	307.5	527
Stress (MPa)	25.93	42.79	59.64	159.54	273.3

Stress on 50,000 Volume Element Sample

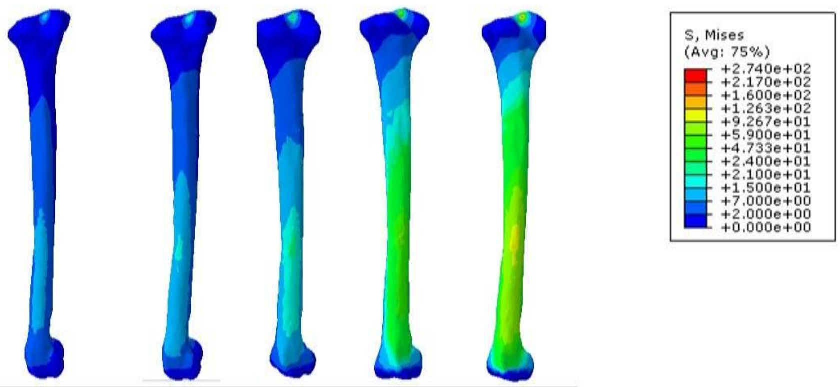

Force (N)	50	82.5	115	307.5	527
Stress (MPa)	25.93	42.79	59.64	159.54	273.3

Stress on 565,000 Volume Element Sample

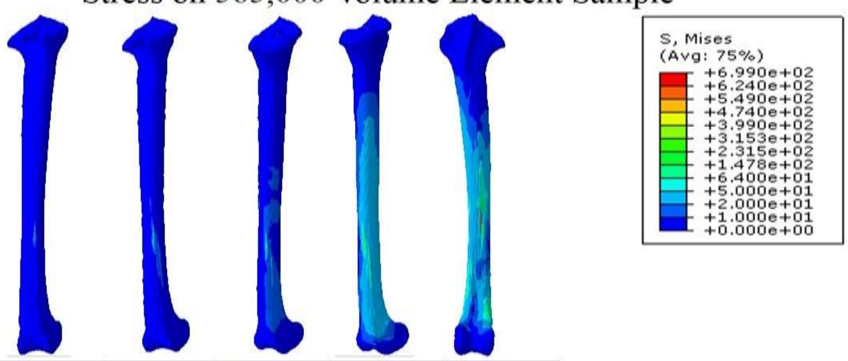

Force (N)	50	82.5	115	307.5	527
Stress (MPa)	64.7	106.8	148.9	398.1	682.2

Applied Force (N)	Healthy Model		Virtually Repaired Model	
	Stress Plot	Stress (N)	Stress Plot	Stress (N)
50		64.72		25.30
82.5	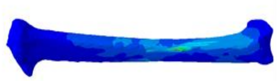	106.80		42.79
115		148.94	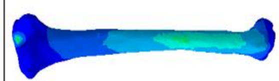	59.64
307.5		398.15		159.54
527	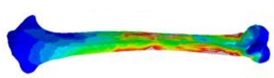	682.26		273.3

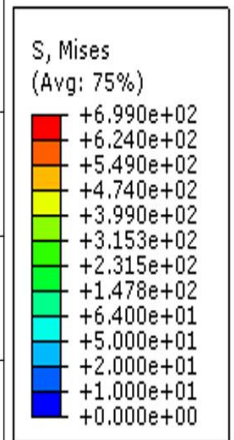

References:

AHMAD, M., NANDA, R., BAJWA, A., CANDAL-COUTO, J., GREEN, S. & HUI, A. 2007. Biomechanical testing of the locking compression plate: when does the distance between bone and implant significantly reduce construct stability? *Injury,* 38**,** 358-364.

BUCEVAC, D., BOSKOVIC, S., MATOVIC, B., ZIVKOVIC, L., VLAJIC, M. & KRSTIC, V. 2007. Correlation between fracture toughness and microstructure of seeded silicon nitride ceramics. *Journal of Materials Science,* 42**,** 7920-7926.

CAMPBELL, G. M., PEÑA, J. A., GIRAVENT, S., THOMSEN, F., DAMM, T., GLÜER, C. C. & BORGGREFE, J. 2017. Assessment of Bone Fragility in Patients With Multiple Myeloma Using QCT-Based Finite Element Modeling. *Journal of Bone and Mineral Research,* 32**,** 151-156.

CURREY, J. 1988. Strain rate and mineral content in fracture models of bone. *Journal of Orthopaedic Research,* 6**,** 32-38.

GREENSPAN, M., WANG, L. I. & ELLIS, R. Validation and improved registration of bone segmentation using contour coherency. Engineering in Medicine and Biology Society, 2006. EMBS'06. 28th Annual International Conference of the IEEE, 2006. IEEE, 244-247.

JULIASTUTI, E., DIPUTRA, Y. & MAYANTASARI, M. Dental panoramic image analysis on mandibular bone for osteoporosis early detection. Instrumentation Control and Automation (ICA), 2013 3rd International Conference on, 2013. IEEE, 138-143.

KIM, J.-D., LEE, S.-J., PARK, S.-J. & LEE, J.-H. 2011. Variation of microstructure on the fracture surface of dense silicon nitride by laser power in LAM. *Metals and Materials International,* 17**,** 515-519.

KING, C. & BIRCH, W. 2015. *Assessment of Maceration Techniques Used to Remove Soft Tissue from Bone in Cut Mark Analysis*.

KRSTIC, Z. & KRSTIC, V. D. 2012. Silicon nitride: the engineering material of the future. *Journal of Materials Science,* 47**,** 535-552.

LAZ, P. J., STOWE, J. Q., BALDWIN, M. A., PETRELLA, A. J. & RULLKOETTER, P. J. 2007. Incorporating uncertainty in mechanical properties for finite element-based evaluation of bone mechanics. *Journal of biomechanics,* 40**,** 2831-2836.

LEE, E. J., LUEDTKE, J. G., ALLISON, J. L., ARBER, C. E., MERRIWETHER, D. A. & STEADMAN, D. W. 2010. The Effects of Different Maceration Techniques on Nuclear DNA Amplification Using Human Bone. *Journal of Forensic Sciences,* 55**,** 1032-1038.

LEE, S., JEONG, J.-W., LEE, J. W., YOO, D.-S. & KIM, S. Distal radius bone mineral density estimation using the filling factor of trabecular bone in the x-ray Image. Engineering in Medicine and Biology Society, 2006. EMBS'06. 28th Annual International Conference of the IEEE, 2006. IEEE, 1980-1982.

LIAO, N., TAO, X., ZHANG, M. & XUE, W. 2011. Effects of temperature and strain rate on fracture properties of amorphous silicon nitride. *Journal of Materials Science: Materials in Electronics,* 22**,** 1346-1349.

LOPTONLINE 2008. Physical Therapy in Lincoln and Ashland for Hip Issues.

LUO, J., ZHOU, Z., ZHANG, H., MA, R. & HOU, J. 2013. Bone response of broiler chickens (*Gallus gallus domesticus*) induced by corticosterone. *Comparative Biochemistry and Physiology Part A: Molecular & Integrative Physiology,* 164**,** 410-416.

MAIRS, S., SWIFT, B. & RUTTY, G. N. 2004. Detergent: An Alternative Approach to Traditional Bone Cleaning Methods for Forensic Practice. *The American Journal of Forensic Medicine and Pathology,* 25**,** 276-284.

MANN, R. W. & BERRYMAN, H. E. 2012. A method for defleshing human remains using household bleach. *Journal of forensic sciences,* 57**,** 440-442.

MATSUDA, S. 2016. Fracture characteristics of silicon nitride ceramic ball subjected to thermal shock. *Journal of materials science,* 51**,** 5502-5513.

MUKHOPADHYAY, A. K. 2001. Indentation fatigue in silicon nitride, alumina and silicon carbide ceramics. *Bulletin of Materials Science,* 24**,** 105-109.

MUSTANSAR, Z. 2015. *Selection of modelling level of detail for incorporating stress analysis into evolutionary robotics simulations of extinct and extant vertebrates.* University of Manchester.

OFFELE, D., HARBECK, M., DOBBERSTEIN, R. C., VON WURMB-SCHWARK, N. & RITZ-TIMME, S. 2007. Soft tissue removal by maceration and feeding of Dermestes sp.: impact on morphological and biomolecular analyses of dental tissues in forensic medicine. *International journal of legal medicine,* 121**,** 341-348.

REILLY, D. T. & BURSTEIN, A. H. 1974. The mechanical properties of cortical bone. *JBJS,* 56**,** 1001-1022.

REILLY, D. T. & BURSTEIN, A. H. 1975. The elastic and ultimate properties of compact bone tissue. *Journal of biomechanics,* 8**,** 393-405.

RUBIN, M., COSMAN, F., LINDSAY, R. & BILEZIKIAN, J. 2002. The anabolic effects of parathyroid hormone. *Osteoporosis international,* 13**,** 267-277.

SCIENCES, S. O. B. A. C. 2002. *Biological safety* [Online]. Available: https://www.qmul.ac.uk/sbcs/internal/healthsafety/biological/.

SEDLIN, E. D. & HIRSCH, C. 1966. Factors affecting the determination of the physical properties of femoral cortical bone. *Acta Orthopaedica Scandinavica,* 37**,** 29-48.

SHASTAK, Y., WITZIG, M., HARTUNG, K., BESSEI, W. & RODEHUTSCORD, M. 2012. Comparison and evaluation of bone measurements for the assessment of mineral phosphorus sources in broilers1, 2. *Poultry Science,* 91**,** 2210-2220.

SHUKLA, P. P. & LAWRENCE, J. 2010. Fracture toughness modification by using a fibre laser surface treatment of a silicon nitride engineering ceramic. *Journal of Materials Science,* 45**,** 6540-6555.

SIMONSEN, K. P., RASMUSSEN, A. R., MATHISEN, P., PETERSEN, H. & BORUP, F. 2011. A Fast Preparation of Skeletal Materials Using Enzyme Maceration*. *Journal of Forensic Sciences,* 56**,** 480-484.

SONG, Y., WANG, S., CHAN, M., CHANDRA, B., DHAWAN, A. & SONG, Y. Femoral fracture risk assessment after intensity modulated radiation therapy (IMRT) for the treatment of soft tissue sarcoma using a novel mathematical model. Engineering in Medicine and Biology Society, 2006. EMBS'06. 28th Annual International Conference of the IEEE, 2006. IEEE, 95-98.

STEADMAN, D. W., DIANTONIO, L. L., WILSON, J. J., SHERIDAN, K. E. & TAMMARIELLO, S. P. 2006. The Effects of Chemical and Heat Maceration Techniques on the Recovery of Nuclear and Mitochondrial DNA from Bone*. *Journal of Forensic Sciences,* 51**,** 11-17.

THURNER, P. J. 2009. Atomic force microscopy and indentation force measurement of bone. *Wiley Interdisciplinary Reviews: Nanomedicine and Nanobiotechnology,* 1**,** 624-649.

TRAN, T. N., LE, L. H., NGUYEN, V.-H., NGUYEN, K.-C. T. & SACCHI, M. D. Sensitivity analysis of leaky lamb modes to the thickness and material properties of cortical bone with soft tissue: A semi-analytical finite element based simulation study. Ultrasonics Symposium (IUS), 2015 IEEE International, 2015. IEEE, 1-4.

VAVVA, M. G., GRIVAS, K. N., CARLIER, A., POLYZOS, D., GERIS, L., VAN OOSTERWYCK, H. & FOTIADIS, D. I. A mechano-regulatory model for bone healing predictions under the influence of ultrasound. Engineering in Medicine and Biology Society (EMBC), 2015 37th Annual International Conference of the IEEE, 2015. IEEE, 921-924.

WERNER, C., LEWANDOWSKI, B., BOPPANA, A. & PENNLINE, J. 2017. Implementation and Integration of a Finite Element Model into the Bone Remodeling Model to Characterize Skeletal Loading.

YAN, J., MECHOLSKY JR, J. J. & CLIFTON, K. B. 2007. How tough is bone? Application of elastic–plastic fracture mechanics to bone. *Bone,* 40**,** 479-484.

YANG, Q., COX, B., NALLA, R. & RITCHIE, R. 2006. Re-evaluating the toughness of human cortical bone. *Bone,* 38**,** 878-887.

ZHANG, M. & FAN, Y. 2014. *Computational biomechanics of the musculoskeletal system*, CRC Press.